LBL-28677
Preprint

Lawrence Berkeley Laboratory

UNIVERSITY OF CALIFORNIA

Materials & Chemical Sciences Division

Submitted to Journal of Chemical Physics

Monte Carlo Simulations of Hydrophobic Polyelectrolytes. Evidence for a Structural Transition in Response to Increasing Chain Ionization

H.H. Hooper, S. Beltran, A.P. Sassi, H.W. Blanch, and J.M. Prausnitz

March 1990

Prepared for the U.S. Department of Energy under Contract Number DE-AC03-76SF00098.

DISCLAIMER

MONTE CARLO SIMULATIONS OF HYDROPHOBIC POLYELECTROLYTES. EVIDENCE FOR A STRUCTURAL TRANSITION IN RESPONSE TO INCREASING CHAIN IONIZATION

*Herbert H. Hooper, Sagrario Beltran, Alexander P. Sassi, Harvey W. Blanch, and John M. Prausnitz**

Chemical Engineering Department
University of California

and

Materials and Chemical Sciences Division
Lawrence Berkeley Laboratory
1 Cyclotron Road
Berkeley, CA 94720

ABSTRACT

Monte Carlo simulation has been used to study the configurational properties of a lattice-model isolated polyelectrolyte with attractive segment-segment interaction potentials. This model provides a simple representation of a hydrophobic polyelectrolyte. Configurational properties were investigated as a function of chain ionization, Debye screening length, and segment-segment potential. For chains with highly attractive segment-segment potentials (i.e., hydrophobic chains), large, global changes in polymer dimensions were observed with increasing ionization. The transformation from a collapsed chain at low ionization to an expanded chain at high ionization becomes increasingly sharp (i.e., occurs over a smaller range of ionization) with increasing chain hydrophobicity. The ionization-induced structural transitions for this model hydrophobic polyelectrolyte are analogous to pH-induced transitions seen in real polyelectrolytes and gels. These studies suggest a simple explanation for such transitions based on competing hydrophilic and hydrophobic interactions.

This work was supported by the Director, Office of Energy Research, Office of Basic Energy Sciences, Chemical Sciences Division of the U.S. Department of Energy under Contract Number DE-AC03-76SF00098.

*To whom correspondence should be addressed

submitted to J. Chem. Phys., March, 1990

I. INTRODUCTION

Much attention has been directed recently at the solution behavior of polyions containing hydrophobic side groups, i.e., hydrophobic polyelectrolytes. Polyelectrolytes exhibit a rich variety of solution properties. The ionized groups on a polyelectrolyte repel each other, tending to expand the polymer chain. The relative values of system length scales (polymer contour length, distance between ionized groups, and screening length) determine the degree of this expansion. In hydrophobic polyelectrolytes, attractive interactions between hydrophobic groups compete with the repulsive interactions of the bound charges. Due to these competing forces, hydrophobic polyelectrolytes exhibit richer variety of solution properties than do polyelectrolytes without hydrophobic groups.

Polyelectrolytes are particularly important as additives and thickening agents in aqueous solution. Because polyelectrolytes expand in solution, they provide large viscosity enhancement at relatively low concentration. However, moderate concentrations of added electrolyte screen the electrostatic repulsions between ionized monomers, and reduce the degree of polyion expansion. Thus, the value of polyelectrolytes as thickening agents is severly limited in electrolyte solutions. Copolymers containing both hydrophilic and hydrophobic monomers (e.g., hydrophobic polyelectrolytes) have been shown to provide viscosity enhancement at low concentrations in the presence of electrolyte.[1-5] In these hydrophobic-polyelectrolyte solutions, intermolecular hydrophobic associations result in the formation of polymer aggregates; these aggregates maintain increased viscosity, even when the individual chain dimensions decrease (e.g., as a result of increased electrolyte concentration).

For solution-thickening applications, the interactions of primary interest are *interchain* hydrophobic associations. However, *isolated* hydrophobic polyelectrolytes also exhibit interesting solution behavior. Strauss and coworkers[6-8] studied the solution properties of a series of 1-1 copolymers of maleic anhydride and alkyl vinyl ethers. The hydrophobicity of the polymers was controlled by varying the length of the alkyl side groups (from methyl to hexyl), and the degree of chain ionization was varied by changing the system pH. Intrinsic viscosity measurements and titration curves indicate that, for alkyl side groups longer than butyl, increasing chain ionization results in a global transition of the polymer from a compact to an expanded conformation. The less hydrophobic chains (methyl and ethyl side groups) behave like typical polyelectrolytes (expanded conformations) over the entire pH range.

In addition to interesting behavior in dilute and concentrated aqueous solution, hydrophobic polyelectrolytes also exhibit unique properties when crosslinked into a gel network. Siegel and Firestone[9] studied a series of lightly crosslinked polyelectrolyte copolymers

containing (dimethylamino)ethyl methacrylate (DMA) and n-alkyl methacrylate esters (n-AMA) of various alkyl chain lengths. The networks undergo dramatic transitions from a collapsed (hydrophobic) state at high pH (low network ionization) to an expanded (hydrophilic) state at low pH (high degree of ionization). The sharpness and extent of the transition depends on the length of the alkyl side group on the methacrylate ester monomers (i.e., the hydrophobicity of the network).

Structural transitions in hydrophobic polyelectroltyes are of scientific and practical interest. Polymers containing both hydrophilic and hydrophobic groups are analogous to proteins, and coil-globule transitions in these synthetic polymers can be compared with native-to-denatured structural transitions in proteins. Thus, synthetic hydrophobic polyelectrolytes can be used as model systems for investigating some of the factors which induce conformational transitions in biological macromolecules. On a practical level, structural transitions in hydrophobic polyelectrolytes provide a mechanism for promoting large changes in solution properties through small changes in system conditions (e.g., pH). For crosslinked gels, this property change is a dramatic volume transition; Siegel and coworkers are investigating the use of gel pH-induced volume transitions in controlled-release applications[10,11].

Our theoretical understanding and description of structural transitions in polyelectrolytes is limited. Uncharged polymers are known to undergo coil-globule transitions in solution, wherein the transition is induced by a change in temperature or polymer/solvent compatibility[12-15]. Considerable effort has been directed at the study of coil-globule transitions for uncharged polymers, and a reasonable theoretical description of this behavior has been developed[14]. However, polyelectrolytes are considerably more complex than uncharged polymers, and a complete understanding of their conformational behavior has not been obtained.

A few authors have proposed theories for explaining structural transitions in hydrophobic polyelectrolytes[16,17] or hydrophobic polyelectrolyte gels[18]. Manning[17] discusses the relationship between polyelectrolyte structural transitions and counterion condensation. He suggests that a polyion experiences structural rearrangement when the linear charge density for the extended chain passes through a critical value; this critical charge density triggers the onset of counterion condensation and a transition in chain dimensions. Schwarz and Siegel[18] have proposed a theory for describing volume transitions in hydrophobic polyelectrolyte gels. They focus attention on the composition-dependence of the dielectric constant within the gel, and the resulting effect of this dielectric constant on ion hydration.

Several interactions and events may contribute to conformational rearrangement in polyelectrolytes, and these simultaneous events are impossible to decouple experimentally.

Thus, it is difficult to determine experimentally the relative importance of the various factors which may contribute to structural transitions and which have been proposed for describing these transitions. Computer simulation provides a powerful means for examining directly the behavior of controlled systems in which all interactions are specified (and known exactly). Monte Carlo simulation has been applied for studying coil-globule transitions in uncharged polymers[19-22], and has recently been used to study configurational properties of polyelectrolytes[23-27]. However, simulation has not previously been used to study the properties of polymers containing both ionized and hydrophobic groups.

In an earlier paper[27] we used Monte Carlo simulation to examine the configurational properties of isolated, partially-ionized polyelectrolytes on a lattice. Here we report simulation studies for partially-ionized polyelectrolytes containing hydrophobic monomers, i.e., hydrophobic polyelectrolytes. We examine a simplified model of a polyelectrolyte which considers counterions and solvent in a 'smeared' continuum representation. Thus, this work isolates attention on the competition between electrostatic (repulsive) and dispersion-force (attractive) interactions. This work provides 'data' for a well-defined limiting representation of a hydrophobic polyelectrolyte, and allows for determining independently the effect of competing coulombic and attractive interactions on configurational properties.

II. METHOD

A. Model description

The basic features of the model are similar to those of Ref. 27; the primary difference here is the inclusion of short-range (dispersion force) interactions between non-bonded, nearest-neighbor segments. The polyelectrolyte is represented as a self-avoiding walk (SAW) of N-1 steps (N segments) on a cubic lattice; the distance between lattice sites, l, is 2.52 A. Ionized groups are considered to be centered at the segment sites, and are uniformly spaced along the chain. The fraction of monomers which are ionized, λ, is varied from 0 (no charged segments) to 1.0 (all segments ionized).

In the model considered here (as in Ref. 27), variations in λ correspond to changes in the chemical composition of the polymer, i.e., to the insertion or removal of ionized monomers. This provides a useful reference case for examining the effect of competing coulombic and hydrophobic interactions on polyelectrolyte configurational properties. It is also instructive to consider the case where the number of ionizable groups is constant, but the *fractional* ionization of those groups varies (i.e., in correspondence with changes in solution pH); this case is useful for examining the effect of pH on the behavior of

polyelectrolytes with fixed composition. Calculations to examine the effect of pH are now in progress.

The interaction between all pairs of ionized segments is described by a screened Debye-Huckel coulombic potential:[28]

$$u_{ij} = \frac{z_i z_j e^2}{D r_{ij}} exp(-\kappa r_{ij}) \tag{1}$$

where segments i and j carry charges $z_i e$ and $z_j e$, and are separated by a distance r_{ij}. The dielectric constant, D, is taken as that of water at 25°C. Free ions are not included specifically in the simulation; instead, their effect on polyion properties is described through the dependence of the inverse Debye screening length, κ, on electrolyte concentration:[28]

$$\kappa^2 = \frac{4 \pi e^2 N_A \sum_i z_i C_i}{D k T} \tag{2}$$

Here, N_A is Avagadro's number, C_i is the concentration of ionic species i, k is Boltzmann's constant, and T is temperature. As in Ref. 27, we consider the polyelectrolyte at infinite dilution; thus, the sum in Eqn. (2) is over the species of *added* electrolyte, and does not include the charges on the polymer or the counterions.

In addition to electrostatic interactions, we also consider dispersion forces. On a lattice, the distance-dependence of dispersion-force interactions is obtained by considering only interactions between nearest-neighbor segments; segments separated by more than one lattice spacing do not interact through dispersion forces. All pairs of nearest-neighbor, non-bonded polymer segments interact with the potential ε. We consider here $\varepsilon < 0$, i.e., the case where polymer-polymer contacts are favored over polymer-solvent contacts. In Ref. 27, we considered only $\varepsilon = 0$ (i.e., hydrophilic polyelectrolytes); we use the results from that limiting case as a point of departure in this work.

It is important to note that *all* segments on the polymer interact through dispersion-forces, including charged segments. We wish to model a polymer in which the repeating units may contain both ionized and hydrophobic side groups. Within a lattice framework, all side-group interactions are localized on a lattice site, and appear to originate from the same origin. Thus, we lose the aesthetically-desirable physical separation of hydrophobic and ionized-group interactions; however, the model captures the essential physics of the system under consideration.

Self-avoiding walks with attractive ($\varepsilon < 0$) interactions, and *without charge* have been studied by simulation and are known to undergo a collapse of chain dimensions with

decreasing temperature or increasing $|\varepsilon|$[19-22]. Simulation has also been used to study polyelectrolytes in the absence of dispersion-force interactions (i.e, for $\varepsilon = 0$)[23-27]. The inclusion of *both* dispersion-force and electrostatic interactions on a single chain distinguishes this work from previous simulation studies on both uncharged and charged polymers.

The total energy for a given configuration is the sum of electrostatic and non-electrostatic (dispersion-force) contributions:

$$E = E_{el} + E_{nel} \tag{3}$$

The electrostatic energy is the sum of screened-coulombic potentials between all pairs of ionized segments:

$$E_{el} = \sum_{i}^{N-1} \sum_{j=i+1}^{N} u_{ij} \tag{4}$$

where N is the number of chain segments, and u_{ij} is given by Eqn. (1). When either i or j is uncharged, $u_{ij} = 0$. The non-electrostatic energy is

$$E_{nel} = \varepsilon m \tag{5}$$

where m is the number of nearest-neighbor (non-bonded) segment-segment contacts for the configuration.

B. Sampling procedure

Metropolis Monte Carlo[29] was used to sample the configurational space of the polyelectrolyte. This method involves generating successive 'trial' chain configurations, and accepting new configurations based on the probability

$$p_{s+1} = \min\left\{1, \exp(-\Delta E / kT)\right\} \tag{6}$$

where ΔE is the energy change in going from configuration s to trial configuration $s+1$. When a trial move is rejected, the previous configuration is retained and considered as a 'new' state in calculating ensemble averages. Of key importance here is the method used for generating successive chain configurations.

In Ref. 27 we were concerned with *hydrophilic* polyelectrolytes where the polymer conformation varied between that of a random coil and a rigid rod. At these low segment densities, the reptation method[30] is adequate for generating successive, uncorrelated chain configurations. Here we are concerned with *hydrophobic* polyelectrolytes which can form

dense, compact structures as well as extended rod-like conformations. Reptation alone is insufficient for sampling compact, high-density configurations because of the possibility of the chain head or tail becoming 'trapped' in the chain interior. Kolinski et al[20] used a combination of reptation and internal chain movements for studying collapse transitions of uncharged polymers. Here we use a similar procedure for generating successive configurations of hydrophobic polyelectroltyes.

Two types of chain motions are employed: reptation, and 'internal' movements. For reptation movements, one end of the chain is randomly designated as the head, and is advanced (in a random direction) one lattice step to an empty site; the remaining segments advance to follow the head. For internal motions, a chain segment is selected (randomly) and, depending on the segment location and local conformation, one of the three movements in Figure 1 is attempted. If the selected segment is an end bead, the terminal bond can rotate or flip to place the end bead in one of the neighboring lattice cells (Fig. 1a); this terminal-bond rotation does not, in fact, involve internal chain motion. If the selected segment is not an end bead, the possible movements are: cross-corner ('kink-jump') moves involving a 180° flip of an adjacent pair of gauche bonds[31] (Fig. 1b), and 'crankshaft' moves involving a 90° rotation of three adjacent, planar bonds[32] (Fig 1c). All motions are subject to excluded-volume constraints; any move which attempts to place a segment in the same lattice site as an existing segment is rejected.

Reptation and internal motions are attempted in random order according to a preset frequency. This reptation:internal-motion attempt frequency was varied to produce the best sampling efficiencies (low autocorrelations and high acceptance ratios) for different chain densities. At low densities (extended chain configurations), reptation movements alone gave the best results. For dense, compact configurations, a combination of 1:1 reptation:internal-movements gave good results.

Simulations were performed for 40-segment chains at various conditions. For all runs, 2×10^6 chain movements (cycles) were attempted, and chain properties were calculated every 10^4 cycles. Runs were initialized by placing the chain in a staircase configuration, and allowing the system to relax through 5×10^4 cycles before beginning the sampling process. The specific initial conformation used is unimportant, because all memory of this conformation is lost during the relaxation step.

C. Calculated Properties

The size of the polymer coil is characterized by the mean-square end-to-end distance

$$\langle r^2 \rangle = \langle (\mathbf{r}_n - \mathbf{r}_1)^2 \rangle \qquad (7)$$

and by the mean-square radius of gyration

$$<s^2> = \frac{1}{N} < \sum_{i=1}^{N} (\mathbf{r}_i - \mathbf{r}_{cm})^2 > \tag{8}$$

where $\mathbf{r}_i$ is the position vector locating the ith bead (segment) of the chain, $\mathbf{r}_{cm}$ is the vector locating the center of mass of the chain, and < > denotes an ensemble average over a Monte Carlo run.

We report separately the ensemble averages $<E_{el}>$ and $<E_{nel}>$ to identify the relative contributions of electrostatic and non-electrostatic chain energies for different conditions. These energies are calculated by averaging Eqns. (4) and (5) over a simulation run.

III. RESULTS AND DISCUSSION

We studied the behavior of isolated, 40-segment chains as a function of polymer hydrophobicity (ε/kT), chain ionization (λ), and Debye screening length (κ^{-1}). Limited runs for longer chains (not reported here) confirmed that chain length affects only macroscopic system properties (e.g., the magnitude of chain dimensions) and not the qualitative nature of the structural transitions reported here. Tables I-IV present results for chain energies $<E_{el}>$ and $<E_{nel}>$ and chain dimensions $<r^2>$ and $<s^2>$. Dimensionless energy ε/kT was varied from 0 (hydrophilic limit) to -2.0 (highly attractive or hydrophobic potential), and chain ionization was varied from λ = 0 (uncharged chain) to λ = 1 (fully ionized chain). Five values of κ^{-1} were used corresponding to 1:1 electrolyte concentrations of 1.0M (κ^{-1} = 3.04 A), 0.1M (κ^{-1} = 9.62 A), 0.01M (κ^{-1} = 30.4 A), 0.001M (κ^{-1} = 96.2 A), and the unscreened limit of $\kappa^{-1} = \infty$.

We first consider the well-studied case for collapse of an uncharged chain. Figure 2 shows the collapse in reduced end-to-end distance of an isolated, 40-segment chain as a function of ε/kT. For high temperatures (or low $|\varepsilon|$) the chain approaches athermal, self-avoiding-walk conditions and has a random-coil configuration. As temperature decreases (or $|\varepsilon|$ increases), the chain dimensions decrease to form more segment-segment contacts; at ε/kT = -2.0, the chain is in a highly compact conformation. The transition in Figure 2 from a random coil to a collapsed configuration is gradual. Other simulation studies on uncharged polymers indicate that an increase in chain length[19,21] or an increase in stiffness of the chain backbone[20] leads to a more dramatic coil-globule transition.

We now consider the behavior of ionized hydrophobic chains. Figure 3 presents the effect of ionization on the reduced end-to-end distance of chains with varying

hydrophobicity. We consider in Figure 3 the case $\kappa^{-1} = \infty$ because the structural transitions of interest here are most readily seen in this unscreened limit; we consider later the effect of screening length on chain behavior. The 'hydrophilic' polyelectrolyte ($\varepsilon/kT = 0$) result of Ref. 27 is included in Figure 3 for comparison; in this limit, the chain expands gradually from a random coil at $\lambda = 0$ to a rigid rod ($\langle r^2 \rangle/(N-1)^2 l^2 = 1$) at $\lambda = 1$. For increasingly hydrophobic chains, the $\lambda = 0$ limit is a more compact conformation, and the transformation of chain dimensions to the rigid-rod limit (reached for all chains at $\lambda = 1$) is less gradual. For sufficiently hydrophobic chains, most of the change in polymer dimensions occurs over a small range of chain ionization. The $\varepsilon/kT = -2.0$ chain experiences an order-of-magnitude change in end-to-end distance in the range $0.25 < \lambda < 0.33$; outside of this range, chain dimensions vary comparatively little with changes in λ.

Figure 3 indicates the occurance of a conformational transition for highly hydrophobic chains in response to an increase in chain ionization. Evidence for this transition can also be seen in the dependence of the radius of gyration (Figure 4) on chain ionization. Figure 5 shows the dependence of the non-electrostatic component of the chain configurational energy on chain ionization. This non-electrostatic energy is directly related to the number of segment-segment contacts; the large increases in $\langle E_{nel} \rangle$ with increasing ionization correspond to large decreases in the number of segment-segment contacts which occur when the chain unfolds to a less compact structure. These combined observations indicate convincingly that the model polyelectrolytes experience a global structural transition in response to a change in chain ionization.

The results shown in Figures 4-6 consider chain behavior in the unscreened limit ($\kappa^{-1} = \infty$). Figure 6 presents the effect of screening length on the reduced end-to-end distance of chains with a constant segment-segment potential of $\varepsilon/kT = -1.0$. Screening length has little effect on the conformation of the collapsed chains; however, increased screening results in reduced chain expansion at high ionizations. Thus, charge-induced conformational transitions become less dramatic as screening (ionic strength) increases. The effect of screening on the conformational transition is most noticable between $\kappa^{-1} = 3.04$ and $\kappa^{-1} = 9.62$ A; at screening lengths larger than $\kappa^{-1} = 9.62$ A (1:1 electrolyte concentrations smaller than 0.1M), the effect of screening-length on the conformational transition is small.

IV. CONCLUSIONS

The Monte Carlo simulations reported here present evidence for ionization-induced structural transitions in model hydrophobic polyelectrolytes. The transitions are continuous in all cases, but become larger and more abrupt with increasing chain hydrophobicity and decreasing charge screening. Theoretical explanations for structural transitions in hydrophobic polyelectrolytes usually consider the transitions to result from counterion condensation[17] or dielectric-dependent hydration effects[18]. An important conclusion from the limiting model considered here is that structural transitions can arise entirely from competing electrostatic (hydrophilic) and dispersion-force (hydrophobic) interactions. Thus, this study suggests a possible alternative explanation for structural transitions in hydrophobic polyelectrolytes based on competing coulombic and hydrophobic interactions.

The charge-induced transitions observed for our model polyelectrolyte appear analogous to pH-induced transitions seen for real hydrophobic polyelectrolytes[6-8] and gels[9]. However, the comparison is not direct because variations in chain ionization here correspond to physical insertion or removal of ionized groups in the model polymer (i.e., a change in polymer composition). For pH-induced transitions, it is therefore important to examine chains with a constant number of ionizable segments and to allow the *fractional* ionization of these segements to vary as dictated by solution pH.

ACKNOWLEDGMENTS

This work was supported by the Director, Office of Energy Research, Office of Basic Energy Sciences, Chemical Sciences Division of the U.S. Department of Energy under contract No. DE-AC03-76SF00098. For fellowship support, S.B. is grateful to the Spanish Ministry of Education and Science (MEC) and A.S. is grateful to the National Science Foundation. The calculations reported here were performed on the IBM 3090 at the U.C. Berkeley Computing Center; we acknowledge with thanks the generous computation time provided by the Computing Center. The authors thank Kevin Mansfield and Doros Theodorou for helpful comments.

REFERENCES

[1]D.N. Schulz, J.J. Kaladas, J.J. Maurer, J. Bock, S.J. Pace, and W.W. Schulz, *Polymer* **28,** 2110 (1987).

[2]C.L. McCormick, T. Nonaka, and C.B. Johnson, *Polymer* **29,** 731 (1988).

[3]P.L. Valint and J. Bock, *Macromolecules* **21,** 175 (1988).

[4]K.T. Wang, I. Iliopoulos, and R. Audebert, *Polym. Bull.* **20,** 577 (1988).

[5]J.C. Middleton, D. Cummins, and C.L. McCormick, *Polymer Preprints* 348 (1989).

[6]P.L. Dubin and U.P. Strauss, *J. Phys. Chem.* **74,** 2842 (1970).

[7]U.P. Strauss, B.W. Barbieri, and G. Wong, *J. Phys. Chem.* **83,** 2840 (1979).

[8]U.P. Strauss, *Macromolecules* **15,** 1567 (1982).

[9]R.A. Siegel and B.A. Firestone, *Macromolecules* **21,** 3254 (1988).

[10]B.A. Firestone and R.A. Siegel, *Proc. Int. Symp. Contr. Rel. Bioact. Mater.* **14,** 81 (1987).

[11]R.A. Siegel, M. Falamarzian, B.A. Firestone, and B.C. Moxley, *J. Controlled Release* **8,** 179 (1988).

[12]P.J. Flory, *Principles of Polymer Chemistry;* Cornell University: Ithaca, NY, 1953.

[13]H. Yamakawa, *Modern Theory of Polymer Solutions;* Harper & Row: NY, 1971.

[14]I.C. Sanchez, *Macromolecules* **12,** 980 (1979).

[15]I.H. Park, Q.W. Wang, and B. Chu, *Macromolecules* **20,** 1965 (1987); B. Chu, I.H. Park, Q.W. Wang, and C. Wu, *Macromolecules* **20,** 2833 (1987).

[16]A.R. Khokhlov, *J. Phys. A* **13,** 979 (1980).

[17]G.S. Manning, *J. Chem. Phys.* **89,** 3772 (1988).

[18]B. Schwarz and R.A. Siegel, work in preparation.

[19]K. Kremer, A. Baumgartner, and K. Binder, *J. Phys. A.* **15,** 2879 (1981).

[20]A. Kolinski, J. Skolnick, and R. Yaris, *J. Chem. Phys.* **85,** 3585 (1986).

[21]N. Karasawa and W.A. Goddard, *J. Phys. Chem.* **92,** 5828 (1988).

[22]H. Meirovitch and H.A. Lim, *J. Chem. Phys.* **91,** 2544 (1989).

[23]C. Brender, M. Lax, and S. Windwer, *J. Chem. Phys.* **74,** 2526 (1981); C. Brender, M. Lax, and S. Windwer, *J. Chem. Phys.* **80,** 886 (1984).

[24]A. Baumgartner, *J. Phys. Lett.* **45,** L-515 (1984).

[25]S.L. Carnie, G.A. Christos, and T.P. Creamor, *J. Chem. Phys.* **89,** 6484 (1988).

[26]G.A. Christos and S.L. Carnie, *J. Chem. Phys.* **91,** 439 (1989).

[27]H.H. Hooper, H.W. Blanch, and J.M. Prausnitz, *Macromolecules* submitted (1990).

[28]P.H. Rieger, *Electrochemistry;* Prentice-Hall: Englewood Cliffs, NJ, 1987.

[29]N. Metropolis, A.W. Rosenbluth, M.N. Rosenbluth, A.H. Teller, and E.J. Teller, *J. Chem. Phys.* **21,** 1087 (1953).

[30]F.T. Wall and F. Mandel, *J. Chem. Phys.* **63,** 4592 (1975).

[31]P.H. Verdier and W.H. Stockmayer, *J. Chem. Phys.* **36,** 227 (1962).

[32]K. Kremer and K. Binder, *Comput. Phys. Rep.* **7,** 259 (1988).

Table I. Electrostatic energy ($<E_{el}>/kT$) of 40-segment partially-ionized polyelectrolytes.

		Ionic strength, M (Concentration of added 1–1 electrolyte)									
ε/kT	NIB[a]	1.0		0.1		0.01		0.001		0[b]	
0	2	0.014	(3)	0.119	(2)	0.291	(3)	0.401	(3)	0.471	(3)
	4	0.176	(3)	0.968	(9)	2.00	(1)	2.69	(2)	3.09	(2)
	8	1.376	(9)	5.57	(4)	10.52	(4)	13.48	(4)	14.84	(8)
	10	2.46	(2)	9.11	(5)	15.9	(1)	20.0	(1)	22.8	(1)
	13	4.99	(3)	16.53	(6)	29.1	(1)	36.8	(1)	42.0	(1)
	20	14.3	(1)	39.8	(1)	65.3	(2)	82.6	(3)	93.2	(3)
	40	78.7	(2)	171.4	(3)	251.9	(3)	310.8	(6)	360.9	(6)
-0.5	2	0.064	(1)	0.259	(3)	0.493	(5)	0.600	(4)	0.666	(4)
	4	0.467	(5)	1.53	(1)	2.75	(2)	3.58	(2)	3.88	(2)
	8	2.22	(2)	6.96	(5)	11.69	(6)	14.47	(7)	15.83	(8)
	10	3.72	(3)	10.40	(5)	16.41	(9)	20.8	(1)	23.2	(1)
	13	6.66	(4)	17.80	(7)	30.1	(1)	37.8	(1)	43.1	(1)
	20	15.06	(7)	39.5	(2)	65.3	(2)	82.7	(2)	93.7	(3)
	40	76.1	(2)	167.9	(3)	250.9	(2)	297	(1)	340	(1)
-1.0	2	0.143	(3)	0.476	(5)	0.751	(6)	0.891	(7)	0.967	(7)
	4	0.886	(6)	2.82	(2)	4.61	(2)	5.32	(2)	5.78	(2)
	8	4.56	(3)	11.8	(1)	16.0	(2)	17.7	(2)	20.2	(2)
	10	7.45	(4)	14.1	(1)	20.0	(1)	24.8	(2)	27.6	(2)
	13	11.5	(1)	20.4	(1)	32.1	(1)	40.3	(1)	43.5	(2)
	20	17.5	(1)	41.0	(1)	66.2	(2)	82.3	(3)	94.5	(3)
	40	77.3	(2)	167.4	(3)	249.0	(3)	318.4	(3)	348	(1)
-1.5	2	0.186	(8)	0.52	(1)	0.81	(1)	0.98	(1)	1.06	(1)
	4	1.06	(1)	3.21	(3)	5.12	(3)	5.92	(3)	6.36	(3)
	8	5.58	(4)	15.85	(8)	23.97	(9)	27.6	(1)	29.7	(1)
	10	9.13	(4)	24.1	(2)	31.7	(4)	36.0	(4)	39.0	(3)
	13	16.51	(9)	28.1	(3)	37.4	(3)	45.1	(3)	49.4	(2)
	20	25.8	(2)	43.6	(2)	67.9	(2)	83.7	(3)	96.6	(3)
	40	79.6	(2)	167.7	(3)	249.6	(3)	308.7	(7)	358.2	(7)
-2.0	2	0.179	(7)	0.60	(2)	0.92	(2)	0.95	(2)	1.04	(2)
	4	1.11	(2)	3.42	(3)	5.43	(5)	6.18	(4)	6.30	(4)
	8	6.02	(5)	17.1	(1)	26.1	(1)	29.29	(9)	31.8	(1)
	10	9.74	(6)	28.3	(1)	41.6	(2)	47.0	(2)	53.0	(1)
	13	18.8	(1)	40.2	(5)	47.1	(4)	53.7	(4)	59.2	(3)
	20	42.6	(3)	51.2	(2)	72.9	(3)	88.4	(3)	99.0	(3)
	40	81.0	(2)	169.8	(3)	250.9	(3)	308.7	(7)	339	(1)

[a]Number of ionized beads. [b]Unscreened coulombic potential between ionized beads. Results in parentheses represent standard errors for last figure shown.

Table II. Non-electrostatic energy ($<E_{nel}>/kT$) of 40-segment partially-ionized polyelectrolytes.

		Ionic strength, M (Concentration of added 1–1 electrolyte)									
ε/kT	NIB[a]	1.0		0.1		0.01		0.001		0[b]	
-0.5	0	-9.08	(5)	-9.08	(5)	-9.08	(5)	-9.08	(5)	-9.08	(5)
	2	-9.01	(5)	-8.73	(6)	-8.69	(6)	-8.66	(6)	-8.66	(5)
	4	-8.49	(6)	-7.52	(6)	-7.12	(5)	-7.06	(9)	-7.09	(6)
	8	-6.43	(6)	-4.35	(5)	-3.51	(4)	-3.44	(4)	-3.39	(4)
	10	-5.58	(5)	-3.05	(3)	-2.45	(3)	-2.33	(3)	-2.34	(4)
	13	-4.18	(4)	-1.94	(2)	-1.42	(2)	-1.32	(1)	-1.32	(2)
	20	-2.14	(2)	-0.67	(2)	-0.372	(6)	-0.337	(5)	-0.328	(5)
	40	-0.172	(5)	-0.009	(1)	-0.0030	(1)	-0.0020	(1)	-0.0020	(1)
-1.0	0	-32.2	(1)	-32.2	(1)	-32.2	(1)	-32.2	(1)	-32.2	(1)
	2	-32.2	(1)	-32.2	(1)	-32.0	(1)	-32.1	(1)	-32.1	(1)
	4	-31.9	(1)	-31.1	(1)	-30.1	(2)	-30.4	(1)	-30.5	(2)
	8	-29.5	(2)	-22.4	(3)	-17.4	(3)	-16.7	(3)	-16.7	(3)
	10	-27.6	(2)	-13.8	(2)	-10.2	(1)	-9.9	(1)	-9.6	(1)
	13	-21.0	(3)	-7.5	(1)	-5.38	(7)	-5.08	(6)	-4.95	(6)
	20	-8.33	(7)	-2.11	(2)	-1.28	(2)	-1.15	(2)	-1.12	(1)
	40	-0.568	(8)	-0.0300	(5)	0.0110	(2)	-0.0070	(3)	-0.0070	(1)
-1.5	0	-57.3	(2)	-57.3	(2)	-57.3	(2)	-57.3	(2)	-57.3	(2)
	2	-56.7	(2)	-56.8	(2)	-56.9	(2)	-56.9	(2)	-56.8	(2)
	4	-56.7	(2)	-56.1	(2)	-56.1	(2)	-56.1	(2)	-55.8	(2)
	8	-56.1	(2)	-53.0	(3)	-52.3	(2)	-52.0	(2)	-52.0	(2)
	10	-54.5	(2)	-47.2	(4)	-37.6	(6)	-35.7	(6)	-34.7	(4)
	13	-51.3	(3)	-24.7	(4)	-16.2	(3)	-15.1	(2)	-14.92	(2)
	20	-26.7	(2)	-5.72	(7)	-3.39	(5)	-2.90	(4)	-2.90	(4)
	40	-1.41	(2)	-0.081	(2)	-0.0240	(5)	-0.0190	(5)	-0.0170	(4)
-2.0	0	-83.3	(2)	-83.3	(2)	-83.3	(2)	-83.3	(2)	-83.3	(2)
	2	-82.2	(2)	-81.5	(2)	-82.4	(2)	-81.6	(3)	-81.5	(2)
	4	-81.8	(3)	-80.6	(2)	-81.8	(2)	-81.4	(3)	-81.5	(2)
	8	-81.1	(3)	-79.0	(3)	-79.1	(3)	-80.5	(4)	-80.4	(3)
	10	-81.5	(2)	-77.8	(3)	-74.1	(4)	-75.3	(5)	-74.8	(4)
	13	-79.3	(3)	-58.0	(8)	-40.5	(5)	-37.1	(6)	-37.3	(5)
	20	-65.4	(5)	-14.3	(2)	-7.9	(1)	-6.88	(9)	-6.79	(9)
	40	-3.29	(4)	-0.177	(3)	-0.058	(1)	-0.040	(1)	-0.0390	(7)

Table III. Reduced mean-square end-to-end distance ($\langle r^2 \rangle / (N-1)^2 l^2$) of 40-segment polyelectrolytes.

		Ionic strength, M (Concentration of added 1–1 electrolyte)									
ε/kT	NIB[a]	1.0		0.1		0.01		0.001		0[b]	
0	0	0.0563	(6)	0.0563	(6)	0.0563	(6)	0.0563	(6)	0.0563	(6)
	2	0.0576	(4)	0.0585	(7)	0.0592	(7)	0.0601	(7)	0.0589	(7)
	4	0.0597	(7)	0.0670	(8)	0.0731	(9)	0.0723	(9)	0.073	(1)
	8	0.0681	(6)	0.094	(1)	0.115	(1)	0.121	(1)	0.124	(2)
	10	0.0721	(9)	0.111	(2)	0.146	(2)	0.149	(2)	0.155	(2)
	13	0.085	(1)	0.141	(2)	0.187	(2)	0.200	(2)	0.204	(2)
	20	0.103	(2)	0.222	(3)	0.317	(4)	0.374	(5)	0.404	(5)
	40	0.176	(2)	0.548	(9)	0.898	(2)	0.919	(1)	0.922	(1)
-0.5	0	0.0261	(3)	0.0261	(3)	0.0261	(3)	0.0261	(3)	0.0261	(3)
	2	0.0263	(3)	0.0276	(3)	0.0281	(5)	0.0281	(4)	0.0283	(3)
	4	0.0290	(5)	0.0358	(5)	0.0391	(5)	0.0409	(7)	0.0407	(5)
	8	0.0421	(6)	0.071	(1)	0.093	(1)	0.097	(1)	0.100	(1)
	10	0.0489	(6)	0.096	(1)	0.125	(1)	0.133	(2)	0.132	(2)
	13	0.062	(1)	0.125	(2)	0.174	(2)	0.189	(2)	0.187	(2)
	20	0.097	(2)	0.204	(2)	0.317	(3)	0.362	(5)	0.383	(5)
	40	0.174	(1)	0.610	(8)	0.897	(1)	0.918	(1)	0.924	(1)
-1.0	0	0.0085	(1)	0.0085	(1)	0.0085	(1)	0.0085	(1)	0.0085	(1)
	2	0.0085	(1)	0.0084	(1)	0.0083	(1)	0.0086	(1)	0.0086	(1)
	4	0.0085	(1)	0.0091	(2)	0.0090	(3)	0.0097	(2)	0.0092	(2)
	8	0.0109	(3)	0.026	(1)	0.045	(1)	0.054	(1)	0.048	(1)
	10	0.0135	(4)	0.060	(1)	0.091	(2)	0.097	(2)	0.100	(2)
	13	0.0244	(8)	0.105	(2)	0.155	(2)	0.161	(2)	0.169	(2)
	20	0.078	(1)	0.200	(3)	0.317	(4)	0.370	(4)	0.371	(4)
	40	0.171	(2)	0.625	(7)	0.894	(1)	0.922	(1)	0.920	(1)
-1.5	0	0.0055	(1)	0.0055	(1)	0.0055	(1)	0.0055	(1)	0.0055	(1)
	2	0.0054	(1)	0.0056	(1)	0.0055	(1)	0.0056	(1)	0.0057	(1)
	4	0.0056	(1)	0.0058	(1)	0.0059	(1)	0.0056	(1)	0.0077	(1)
	8	0.0057	(2)	0.0073	(3)	0.0073	(3)	0.0078	(3)	0.0077	(3)
	10	0.0064	(2)	0.0127	(6)	0.029	(1)	0.038	(2)	0.036	(1)
	13	0.0070	(3)	0.061	(2)	0.112	(2)	0.123	(2)	0.120	(2)
	20	0.0430	(7)	0.185	(2)	0.301	(4)	0.352	(5)	0.352	(4)
	40	0.171	(3)	0.614	(7)	0.908	(1)	0.923	(1)	0.923	(1)
-2.0	0	0.0041	(1)	0.0041	(1)	0.0041	(1)	0.0041	(1)	0.0041	(1)
	2	0.0052	(2)	0.0051	(2)	0.0053	(2)	0.0046	(2)	0.0045	(1)
	4	0.0041	(1)	0.0054	(2)	0.0050	(2)	0.0048	(2)	0.0045	(2)
	8	0.0045	(1)	0.0035	(2)	0.0045	(1)	0.0050	(2)	0.0046	(2)
	10	0.0045	(2)	0.0052	(3)	0.0054	(3)	0.0063	(4)	0.0065	(2)
	13	0.0048	(2)	0.022	(1)	0.058	(2)	0.075	(2)	0.070	(2)
	20	0.0115	(5)	0.153	(2)	0.277	(4)	0.331	(4)	0.337	(4)
	40	0.161	(2)	0.604	(9)	0.894	(1)	0.921	(1)	0.920	(1)

Table IV. Reduced mean-square radius of gyration ($\langle s^2 \rangle / (N-1)l^2$) of 40-segment polyelectrolytes.

		Ionic strength, M (Concentration of added 1–1 electrolyte)									
ε/kT	NIB[a]	1.0		0.1		0.01		0.001		0[b]	
0	0	0.349	(3)	0.349	(3)	0.349	(3)	0.349	(3)	0.349	(3)
	2	0.355	(2)	0.359	(3)	0.366	(4)	0.367	(3)	0.363	(3)
	4	0.367	(3)	0.400	(4)	0.427	(4)	0.425	(4)	0.427	(5)
	8	0.409	(3)	0.521	(6)	0.613	(5)	0.637	(5)	0.650	(7)
	10	0.426	(4)	0.604	(7)	0.740	(9)	0.753	(8)	0.778	(9)
	13	0.489	(4)	0.742	(7)	0.926	(8)	0.98	(1)	0.991	(8)
	20	0.583	(7)	1.06	(1)	1.44	(2)	1.64	(2)	1.78	(2)
	40	0.914	(9)	2.42	(3)	3.31	(1)	3.34	(1)	3.35	(1)
-0.5	0	0.190	(2)	0.190	(2)	0.190	(2)	0.190	(2)	0.190	(2)
	2	0.192	(2)	0.201	(2)	0.203	(2)	0.205	(2)	0.205	(2)
	4	0.206	(2)	0.243	(3)	0.261	(2)	0.270	(4)	0.268	(3)
	8	0.275	(3)	0.413	(5)	0.519	(6)	0.533	(6)	0.545	(7)
	10	0.310	(3)	0.530	(5)	0.658	(6)	0.691	(7)	0.685	(7)
	13	0.379	(5)	0.676	(7)	0.883	(9)	0.940	(9)	0.933	(9)
	20	0.543	(7)	0.995	(8)	1.44	(1)	1.61	(2)	1.69	(2)
	40	0.903	(5)	2.51	(2)	3.304	(4)	3.346	(2)	3.353	(2)
-1.0	0	0.0962	(5)	0.0962	(5)	0.0962	(5)	0.0962	(5)	0.0962	(5)
	2	0.0966	(4)	0.0967	(6)	0.0975	(5)	0.0971	(6)	0.0973	(7)
	4	0.0982	(5)	0.1029	(8)	0.104	(1)	0.107	(1)	0.106	(1)
	8	0.111	(2)	0.196	(6)	0.298	(7)	0.346	(7)	0.310	(7)
	10	0.124	(2)	0.365	(6)	0.519	(8)	0.547	(8)	0.554	(8)
	13	0.191	(4)	0.595	(8)	0.816	(9)	0.84	(1)	0.882	(9)
	20	0.452	(5)	0.991	(9)	1.45	(2)	1.66	(2)	1.67	(2)
	40	0.898	(6)	2.56	(2)	3.296	(4)	3.350	(3)	3.343	(3)
-1.5	0	0.0809	(3)	0.0809	(3)	0.0809	(3)	0.0809	(3)	0.0809	(3)
	2	0.0823	(3)	0.0823	(3)	0.0819	(4)	0.0814	(3)	0.0821	(4)
	4	0.0821	(3)	0.0835	(5)	0.0828	(4)	0.0831	(4)	0.0835	(4)
	8	0.0832	(4)	0.0908	(9)	0.094	(1)	0.095	(1)	0.095	(1)
	10	0.0863	(6)	0.124	(3)	0.228	(8)	0.268	(9)	0.254	(6)
	13	0.096	(1)	0.395	(9)	0.65	(1)	0.70	(1)	0.698	(9)
	20	0.288	(4)	0.94	(1)	1.41	(2)	1.62	(2)	1.61	(2)
	40	0.89	(1)	2.53	(2)	3.313	(4)	3.349	(3)	3.347	(3)
-2.0	0	0.0756	(2)	0.0756	(2)	0.0756	(2)	0.0756	(2)	0.0756	(2)
	2	0.0766	(2)	0.0768	(2)	0.0764	(2)	0.0761	(3)	0.0764	(2)
	4	0.0772	(3)	0.0774	(3)	0.0774	(3)	0.0765	(2)	0.0771	(3)
	8	0.0779	(3)	0.0794	(4)	0.0807	(4)	0.0804	(7)	0.0793	(7)
	10	0.0769	(3)	0.0856	(8)	0.092	(1)	0.095	(2)	0.0870	(8)
	13	0.0794	(4)	0.199	(7)	0.434	(9)	0.53	(1)	0.490	(8)
	20	0.126	(3)	0.82	(1)	1.35	(2)	1.57	(2)	1.60	(2)
	40	0.855	(7)	2.50	(3)	3.297	(4)	3.347	(2)	3.346	(3)

List of Figure Captions

Figure 1. The three types of attempted internal chain motions. Initial configurations are denoted by filled circles (segments) joined by solid lines (bonds); new configurations are denoted by open circles and dashed lines. (a) When the randomly selected bead (bead i) is an end segment, the terminal bond can rotate or flip to place this bead in a neighboring site; (b) When bead i is joined by two 90° bonds, and the lattice site opposite i is not filled by segment $i+2$ or segment $i-2$, the attempted move is a two-bond flip to place i in this opposite lattice site. (c) When i is joined by two 90° bonds and the site opposite i is filled by segment $i+2$ or segment $i-2$, the attempted move is a three-bond *crankshaft* rotation to place bead i and *a neighboring bead* in either of the two locations shown.

Figure 2. Collapse of an uncharged 40-segment chain in response to decreasing temperature or increasing $|\varepsilon|$.

Figure 3. Transitions in the end-to-end dimension of hydrophobic polyelectrolytes induced by an increase in the number of ionized segments. Results are for the unscreened limit ($\kappa^{-1} = \infty$). Curves are drawn to guide the eye.

Figure 4. Transitions in the reduced radius-of-gyration for unscreened hydrophobic polyelectrolytes. Results are analogous to those of Figure 3.

Figure 5. Large increases in $\langle E_{nel} \rangle$ with chain ionization indicate large decreases in the number of segment-segment contacts around the conformational transitions seen in Figures 3 and 4.

Figure 6. Effect of charge screening on structural transitions for chains with $\varepsilon/kT = -1.0$. Ionic strengths indicate the 1:1 electrolyte concentrations corresponding to the screening lengths used in the respective simulations.

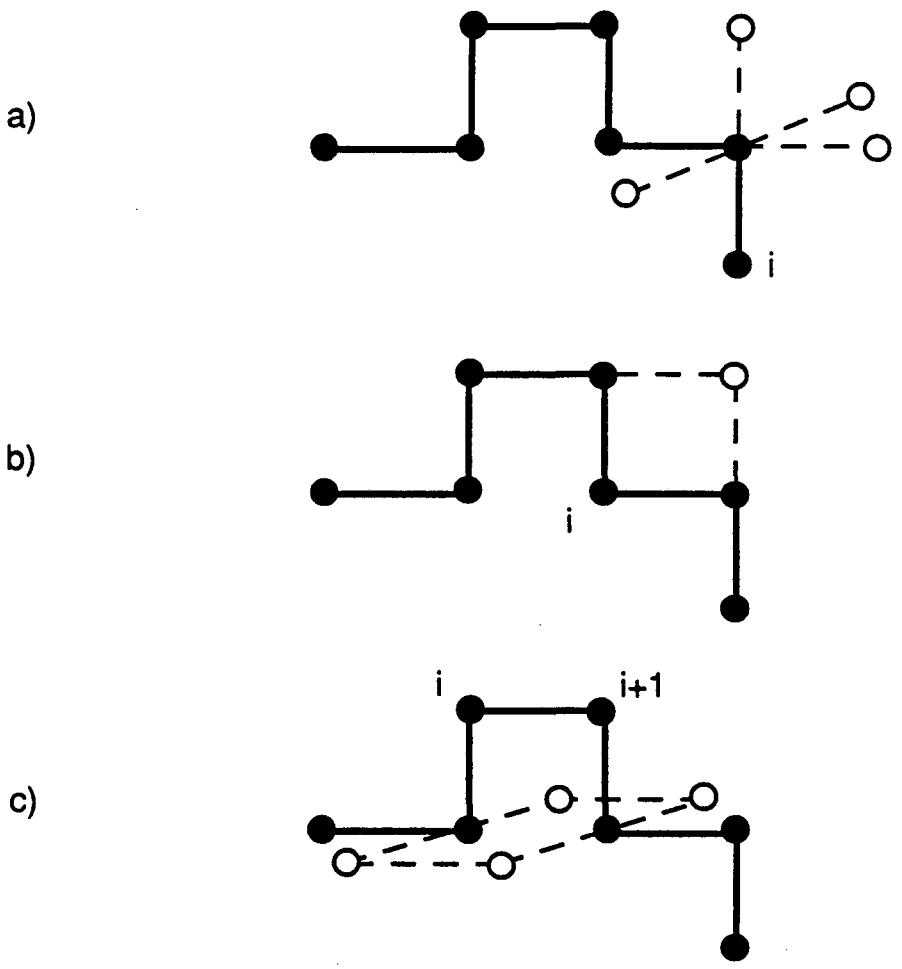

Figure 1

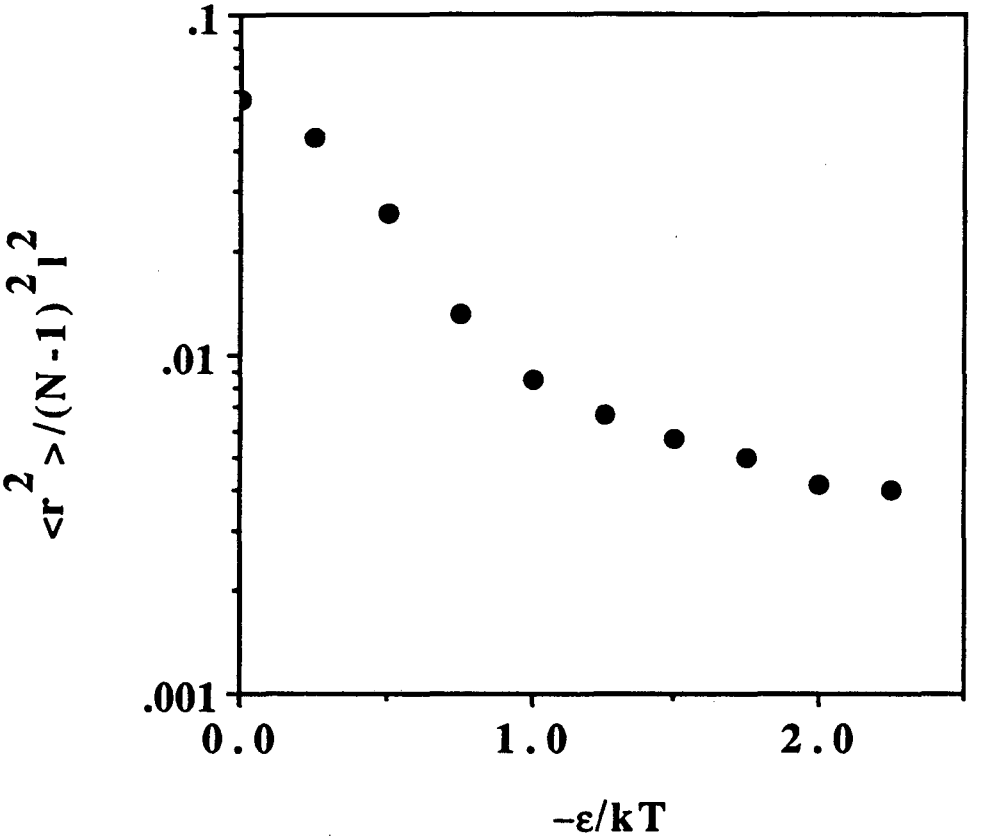

Figure 2

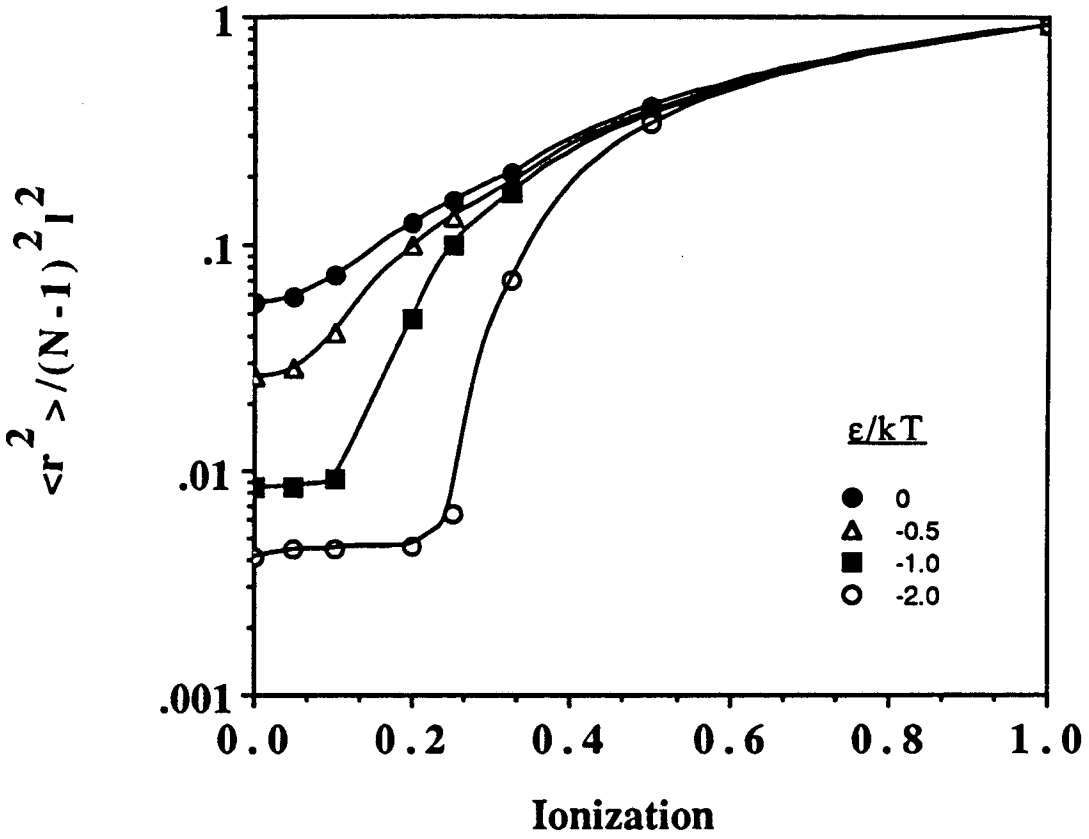
1
.1
.01
.001
0.0
0.2
0.4
0.6
0.8
1.0
Ionization
$\langle r^2 \rangle / (N-1)^2 l^2$
ε/kT
0
-0.5
-1.0
-2.0

Figure 3

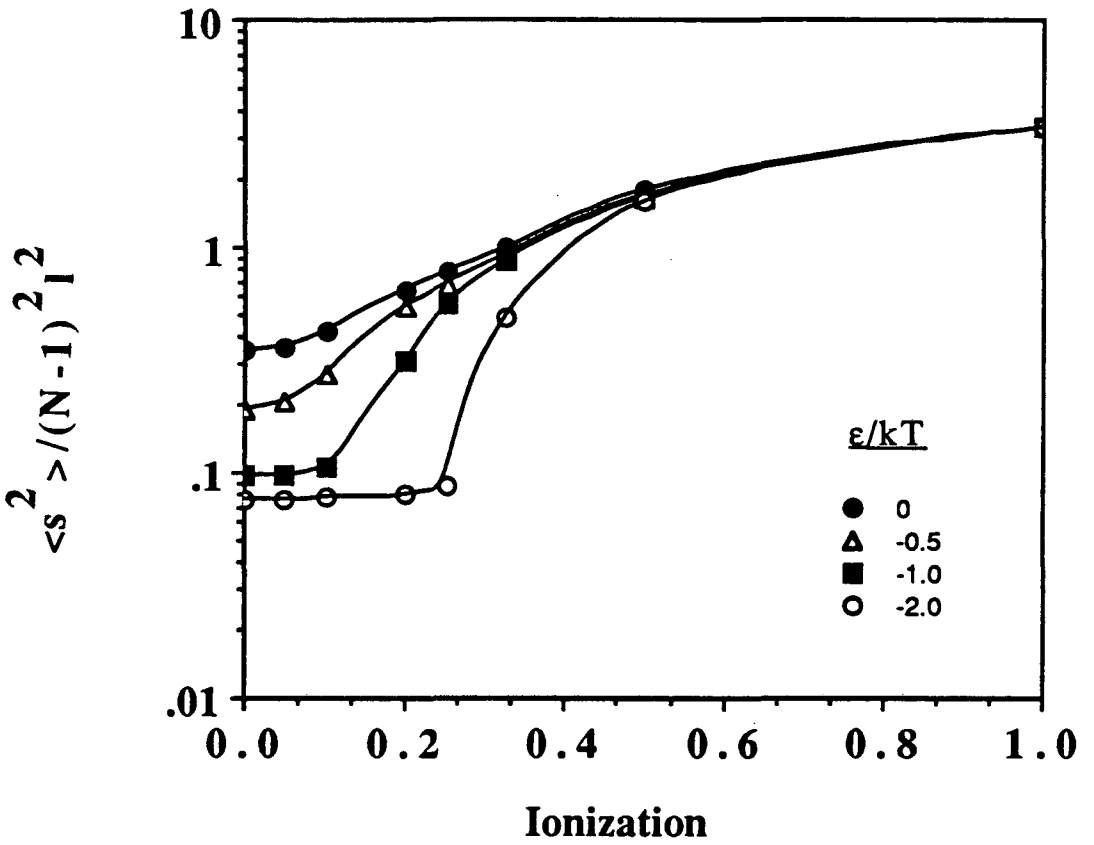
10
1
.1
.01
0.0
0.2
0.4
0.6
0.8
1.0
Ionization
$\langle s^2 \rangle / (N-1)^2 I^2$
ε/kT
0
-0.5
-1.0
-2.0

Figure 4

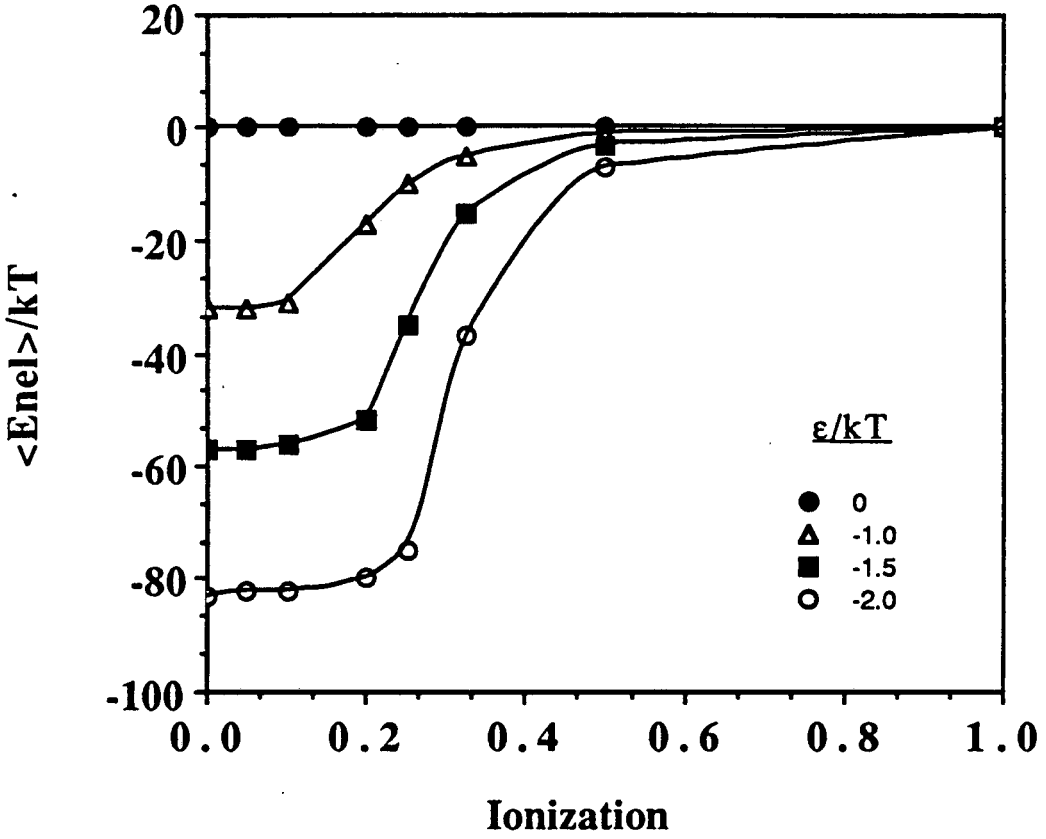
20
0
-20
-40
-60
-80
-100
<Enel>/kT
0.0
0.2
0.4
0.6
0.8
1.0
Ionization
ε/kT
0
-1.0
-1.5
-2.0

Figure 5

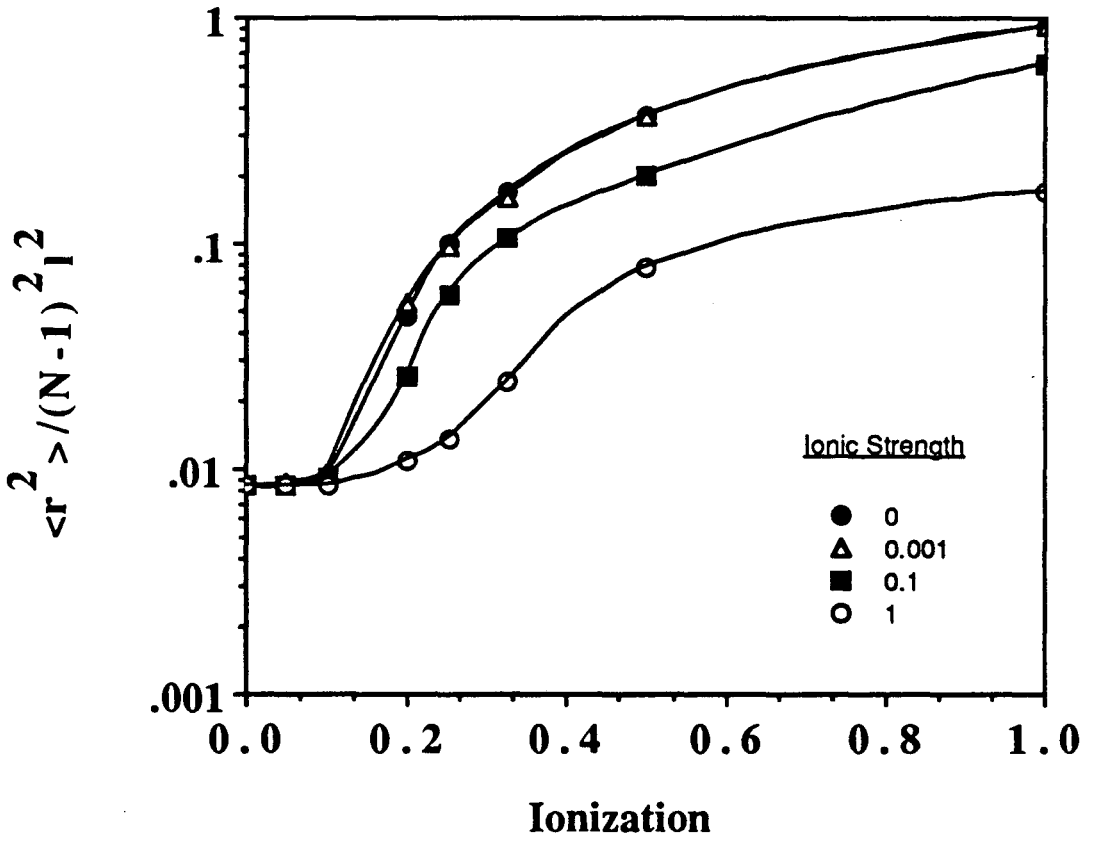
1
.1
.01
.001
0.0
0.2
0.4
0.6
0.8
1.0
Ionization
$\langle r^2 \rangle / (N-1)^2 l^2$
Ionic Strength
0
0.001
0.1
1

Figure 6

LAWRENCE BERKELEY LABORATORY
TECHNICAL INFORMATION DEPARTMENT
1 CYCLOTRON ROAD
BERKELEY, CALIFORNIA 94720